Article

Comparative Study of Cu/ZSM-5 Catalysts Synthesized by Two Ion-Exchange Methods

Dalia Santa Cruz-Navarro [1,*], Miguel Torres-Rodríguez [2], Mirella Gutiérrez-Arzaluz [2], Violeta Mugica-Álvarez [2] and Sibele Berenice Pergher [3]

1   Posgrado en Ciencias e Ingeniería, Universidad Autónoma Metropolitana, Av. San Pablo 180, Azcapotzalco, Mexico City 02200, Mexico
2   Área de Química Aplicada, Departamento de Ciencias Básicas, Universidad Autónoma Metropolitana, Av. San Pablo 180, Azcapotzalco, Mexico City 02200, Mexico; trm@azc.uam.mx (M.T.-R.); gam@azc.uam.mx (M.G.-A.); vma@azc.uam.mx (V.M.-Á.)
3   Departamento de Química, Universidade Federal do Rio Grande do Norte, Av. Senador Salgado Filho, 3000 Centro de Convivência Djalma Marinho Sala 09 S/N Lagoa Nova, Natal 2408102, Brazil; sibelepergher@gmail.com
*   Correspondence: sonysantacruz@gmail.com; Tel.: +52-55-2863-1693

Abstract: As catalysis is one of the pillars of green chemistry, this work aimed at continuing the development of synthesized catalysts under controlled conditions that allow the attainment of materials with the best physicochemical properties for the process for which they were designed. Based on this, the synthesis, characterization, and comparison of copper-based catalysts supported on ammonium and acidic ZSM-5-type zeolite by two ion exchange methods, liquid phase and solid state, are presented. The catalysts obtained were characterized by SEM/EDS, FTIR, XRD, and TPR to study the effect of the synthesis method on the physicochemical properties of each catalyst. The SEM/EDS results showed a homogeneous distribution of copper in the zeolite and the TPR led to determining the temperature ranges for the reduction of $Cu^{2+} \rightarrow Cu^{+} \rightarrow Cu^{0}$. Furthermore, the X-ray results showed no modification of the structure of the zeolite after ion exchange, heat treatment, and TPR analysis.

Keywords: Cu-ZSM-5 catalysts; TPR; green chemistry

1. Introduction

Zeolites are microporous aluminosilicates that exhibit a framework composed by SiO_4 and AlO_4^{-} tetrahedral units [1]. Zeolites have been widely used as catalytic supports and catalysts due to their remarkable properties, such as molecular pore size, regular structure, and chemical and thermal stability, in addition to their ion exchange property, which gives them the ability to exchange their compensation cations for catalytically active metals, tuning their catalytic properties under controlled conditions [2,3]. Likewise, other factors to consider in obtaining zeolite-based catalysts are the preparation methods and the treatment conditions, which exert notable influence on the final properties of the catalysts [4]. Thus, a wide variety of methods have been reported, such as precipitation, impregnation, incipient wet impregnation, and ion exchange in the aqueous phase or in the solid state, among others [5–10]. The ion exchange method in the liquid phase and in the solid phase has shown advantages when exchanging the compensating cations of the zeolites for metal ions. This has led to the achievement of an excellent exchange of the compensating cation of the zeolite with the catalytically active metal ions, thus attaining an excellent amount of the metal within the pores, as well as a good metallic dispersion [10]. Solid-state ion exchange can create some active sites different from those obtained by the classical ion exchange method in the liquid phase [11], which can improve catalytic activity. In this regard, recently Gates et al. [12] and B. Gates [13] have published work on the importance

of atomic dispersion (molecular single-site supported metal catalyst) of metals to improve catalytic activity. Additionally, Chen et al. [14] reported the importance of the metal ligand interaction of platinum atoms, coordinated with the oxygen atoms of MIL-101, which offers alternative routes to improving the selectivity in the hydrogenation of CO_2 to methanol. Additionally, theoretical and experimental studies on solid-phase ion exchange have been published; for example, Chen et al. [15], using calculations based on density functional theory, investigated the use of solid-state ion exchange of copper in zeolites, showing that the formation of a volatile metal complex facilitates the diffusion of the metal complex into the zeolite lattice, thus generating efficient ion exchange at a moderate temperature. The experimental study by Shwan et al. [9] shows the effect of different gaseous atmospheres during the solid-state ionic exchange of copper species in zeolites at 250 °C, obtaining active catalysts for the reduction of NO with NH_3, (NH_3-SCR). Additionally, Zhang et al. [16] have reported the use of solid-state ion exchange in the synthesis of dimethyl carbonate, using different types of zeolite: Cu-Y, Cu-ZSM-5, and Cu-MOR. Copper-based catalysts are interesting because of their low cost and their proven activity for oxidation-reduction reactions. Furthermore, the catalysts are mainly considered a pillar of green chemistry [17] and a basic element of sustainable processes.

Therefore, the objective of the present work is to carry out a comparative study of the physicochemical properties of Cu-ZSM-5 catalysts synthesized by two ion exchange methods, liquid phase (LPIE) and solid state (SSIE), SEM/EDS, FTIR, XRD, and TPR were used to verify if there were differences in the properties, to take them into account appropriately. The intention is to evaluate these catalysts in the transformation of CO_2 to products of added value forming a Cu-ZnO/Cu-zeolite-base hybrid catalyst and with the Cu-ZSM-5 catalysts to evaluate the oxidation of methane to methanol.

2. Materials and Methods

Commercial ammonium ZSM-5 zeolite, "Alfa Aesar, Ward Hill, MA, USA" SiO_2/Al_2O_3 at 30:1 molar ratio was used for the synthesis of the catalysts. The copper precursor salt was $Cu(NO_3)_2 \cdot H_2O$, 98%, "Sigma Aldrich, St. Louis, MA, USA". The ion exchange was carried out in both the solid-state and in the liquid phase, with the ammonium and acid zeolite forms.

2.1. Zeolite in Acid Form (H-ZSM-5)

To obtain the zeolite in acid form (H-ZSM-5), a sample of the ammonium zeolite ZSM-5 was calcined in a tube furnace (Thermolyne 21100 model, Dubuque, IA, USA) at 550 °C for 3 h, with a heating ramp of 5 °C/min under a nitrogen atmosphere.

2.2. Liquid Phase Ion Exchange (LPIE)

A sample of 1.0 g ZSM-5 zeolite was mixed with 15 mL of a 0.1 M solution of $Cu(NO_3)_2 \cdot H_2O$ in a rotary evaporator at 60 °C for 3 h at 160 rpm. Three ion exchange cycles were performed, with abundant deionized water washing followed by a drying step between each exchange at 80 °C for 12 h.

2.3. Solid-State Ion Exchange (SSIE)

The zeolite (1.0 g) was mixed with $Cu(NO_3)_2 \cdot H_2O$ salt (0.12 g) in an agate mortar. Subsequently, the mixture was placed in a quartz reactor and heated at 500 °C for 5 h, with a heating ramp of 5 °C/min in 5% NH_3/Ar, PRAXAIR at a constant flow of 15 mL/min.

2.4. Characterization

The catalysts were characterized by XRD, SEM/EDS, FTIR, and TPR.

The diffraction pattern of the catalysts was obtained through a Philips X-Ray Diffractometer (XRD), model X'Pert, in order to perform a qualitative analysis (phase identification). The diffractometer was fitted with a copper anode tube using K_α radiation and with

an incident monochromator with $\lambda = 1.5406$ Å, a 2 theta range from 4.0° to 80°, a step size of 0.02°, and a step time of 2.5 s.

The morphological analysis of the catalysts was performed by Variable Pressure Scanning Electron Microscopy (SEM), Carl Zeiss instrument model Supra 55VP, and the elemental chemical analysis was performed by energy dispersive spectroscopy (SEM/EDS) using an Oxford detector.

The Fourier Transform Infrared Spectroscopy (FTIR) analysis was performed with a Varian spectrometer, Excalibur 3600 model, and the analysis was carried out by Attenuated Total Reflectance (ATR) with a range from 400 to 4000 cm^{-1} in the mid-infrared region.

The Temperature-Programmed Reduction (TPR) analysis was performed on a Bel Japan TPD/TPR/TPO analyzer, BelCat model, with two stages of pretreatment and reduction with hydrogen flow, using a quartz micro-reactor.

Pre-treatment: 70 mg of previously dried sample were weighed and heated at a rate of 10 °C/min until reaching 350 °C in an oxygen atmosphere (5% O_2/He, 50 cm^3 min^{-1}) for 30 min, and subsequently the sample was cooled in an Ar flow (50 cm^3 min^{-1}) to 50 °C, for 10 min with Ar flow.

Thermo reduction: With a heating ramp from 10 °C/min to 700 °C with a flow of reducing gas (5% H_2/Ar) of 40 cm^3 min^{-1}, the atmosphere and temperature were maintained for 30 min.

3. Results

Four catalysts were obtained as reported in Table 1.

Table 1. ZSM-5 zeolite supported copper catalysts.

Zeolite	Form	Ion Exchange	Catalyst
ZSM-5 molar ratio SiO_2/Al_2O_3 30:1	Ammonium	Liquid phase	ZA3L1
		Solid-state	ZA3S4
	Acid	Liquid phase	ZH3L1
		Solid-state	ZH3S3

3.1. XRD

In Figure 1a,b, the X-ray powder diffraction patterns display the typical lines of the ZSM-5 zeolite that can be clearly identified [18]. The zeolite acid solid-state (ZH3S3) catalyst shows the characteristic lines of metallic copper located at 2θ = 43.3, 50.4, and 74.1°, which correspond to planes (111), (200), and (220) [19,20]. This result suggests the presence of copper nanoparticles, due to the synthesis method which used a physical mixture of the precursor salt of copper with the zeolite, which is corroborated by the SEM results, of Section 3.1. In contrast to this result, the other catalysts do not present these diffraction lines, so copper is considered to be located within the pores and channels of the parent zeolite, out of the reach of the incident beam, after it was exchanged for the ammonium ion or, in the case of acidic zeolites, for the proton, forming a metal complex inside the channels [21]. Furthermore, it is important to highlight that the change in the intensity of the diffraction lines at low angles is more important for the samples synthesized by ionic exchange in solid state, compared to those from ionic exchange in the liquid phase. It is important to note that, the ion exchange method allows the exchange of the ammonium ion or the proton of the zeolite for the Cu^{2+} ions, leaving this ion tetrahedrally coordinated to the aluminum of the network that forms the zeolite channels [22].
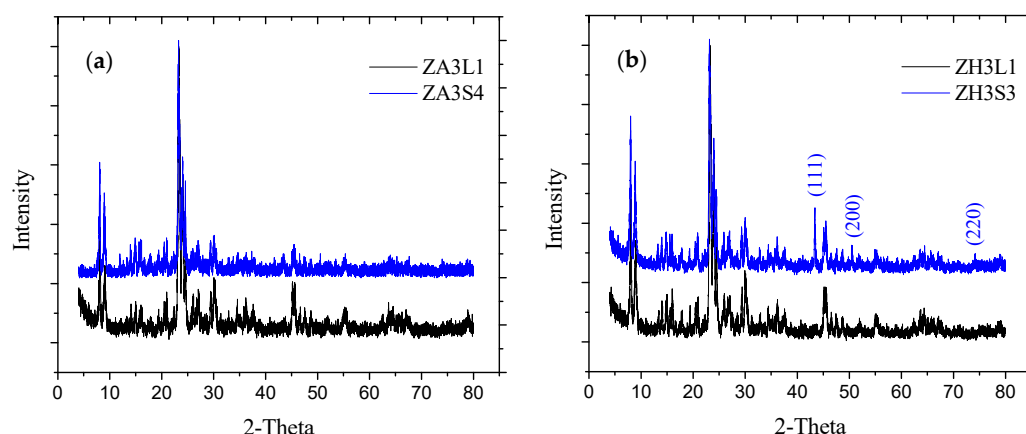
Figure 1. (**a**) Diffraction pattern of the catalysts ZA3L1 and ZA3S4; (**b**) Diffraction pattern of the catalysts ZH3L1 and ZH3S3.

3.2. SEM/EDS

Based on the results of the EDS analyses performed in triplicate (Figure 2), the catalysts obtained with the zeolite in acid form presented lower copper content than those of the ammonium zeolite. In addition, the catalysts obtained by SSIE displayed higher copper content than those obtained by LPIE.
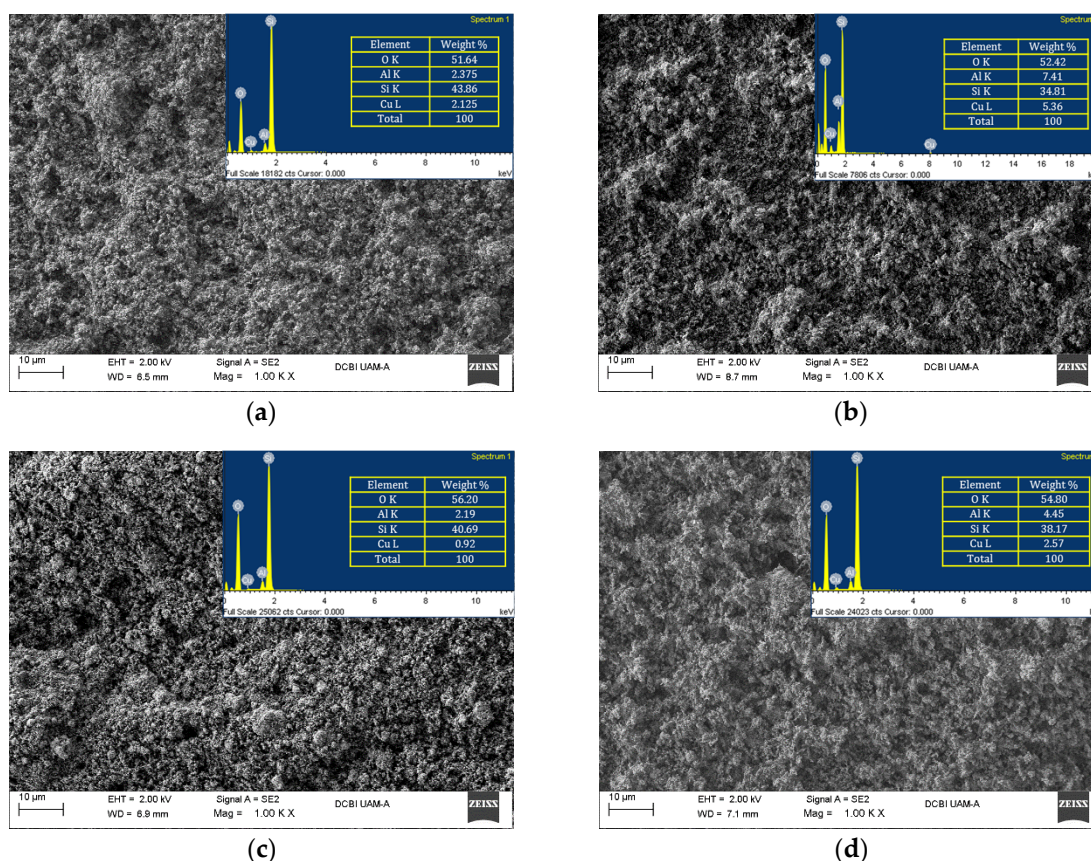

Figure 2. Micrographs and EDS analysis of the catalysts (**a**) ZA3L1, (**b**) ZA3S4, (**c**) ZH3L1, and (**d**) ZH3S3 that establish the overall granular morphology attained for each case.

The %w Cu in ZA3S4 (5.36%) > ZH3S3 (2.57%) > ZA3L1 (2.125%) > ZH3L1 (0.92%).

This difference in metal charge is attributed to the fact that SSIE facilitates the diffusion of the volatile metal complex into the zeolite pores when ion exchange is carried out at high

temperature (500 °C) [9,11], which resulted in a more efficient exchange of the copper ion in the cationic centers located in the internal structure of the zeolite, and the achievement of a homogeneous metallic complex, as has recently been suggested [15].

In addition, in Figure 2 the SEM micrographs of the catalysts at a magnification of 1000× are presented, exhibiting nano-sized, homogeneous, irregularly shaped particles. Moreover, Figure 3 shows the elemental mapping of the ZA3S4 catalyst, in which the elements comprising it and their relative weight % are shown in tabular form in each inset. In the case of copper, the active catalyst phase shows a good distribution and dispersion of the metal in the zeolite, which indicates that the ion exchange method allowed a homogeneous metal distribution.
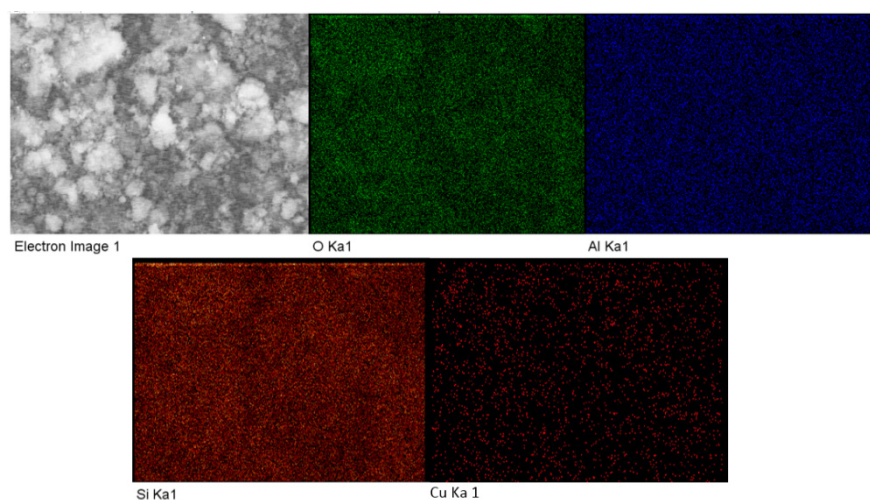

Figure 3. SEM secondary electron image of the ZA3S4 catalyst and four elemental mappings of the elements comprised.

3.3. FTIR

In Figure 4a, the IR spectra of the catalysts ZA3L1 and ZA3S4 are shown, and in Figure 4b, the IR spectra of the catalysts ZH3L1 and ZH3S3 are shown. In the spectra, only the characteristic absorption bands of the zeolites are observed, indicating the absence of elements or compounds foreign to the structure of the support after ion exchange with both methods, liquid phase and solid phase. The type of vibration assigned to each absorption band of the support is shown in Table 2.
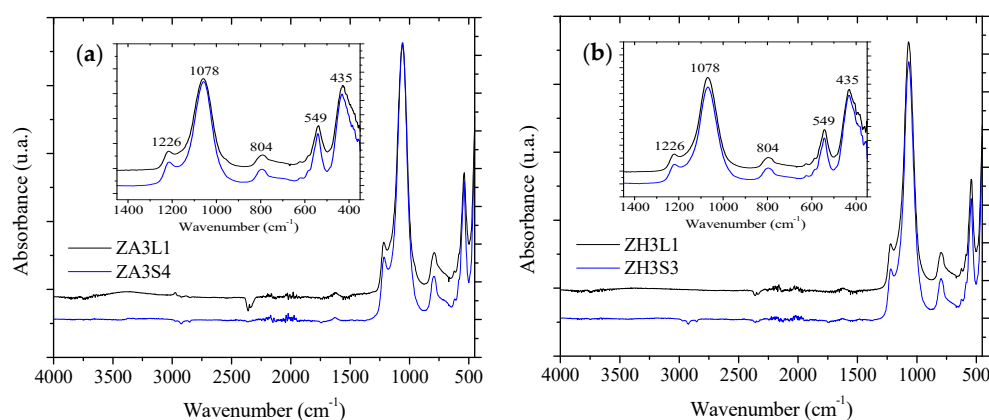

Figure 4. FTIR spectra of catalysts (**a**) ZA3L1 and ZA3S4, (**b**) ZH3L1 and ZH3S3, in the region of 4000 to 450 cm^{-1}.

Table 2. Type of vibrations identified in the FTIR spectrum of the catalysts [23,24].

Wave Number (cm^{-1})	Vibration Type
1226	External Asymmetric stretch (TO$_4$)
1078	Internal Asymmetric stretch (TO$_4$)
804	External Symmetrical stretch (TO$_4$)
549	External External link vibrations (TO$_4$)
435	Internal Bending of the tetrahedral (TO$_4$)
TO$_4$: Tetrahedral TO$_4$ (T = Si o Al)	

3.4. H$_2$-TPR

Figure 5a,b show the hydrogen reduction thermograms of the four catalysts, reported in Table 1. The reduction peaks for each catalyst were identified by the numbers in the thermograms. Three reduction peaks appear in the case of the catalysts obtained from zeolite in ammonium form (Figure 5a), whose presence has been reported for Cu/Zeolite ZSM-5 catalysts obtained by SSIE [25]. The reduction profiles of these two catalysts are similar to one another, except for the lag in reduction temperatures. For the catalysts obtained with zeolite in acid form, there were two reduction peaks (Figure 5b), which have also been reported and identified [26]; it is straightforward that the reduction profiles of these two catalysts are different from each other. The shape and position of the peaks vary and depend on the dispersion of Cu and the interaction with the zeolite matrix, as reported by Bulánek et al. [21].
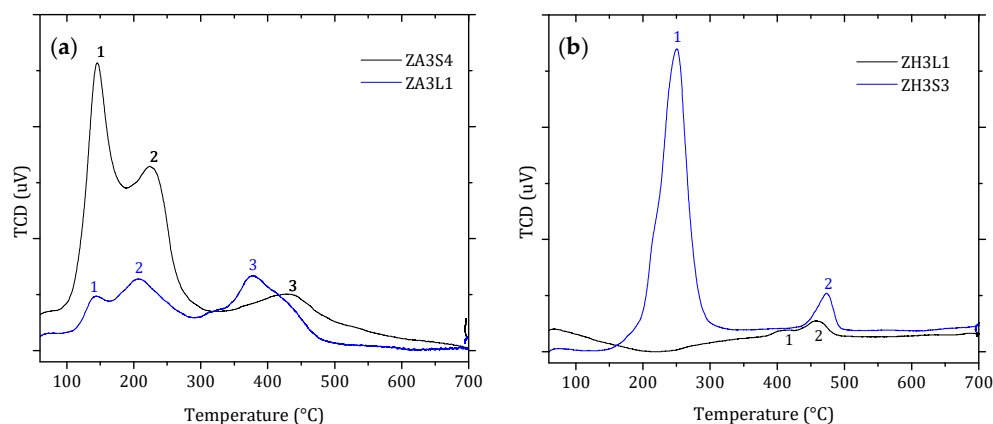

Figure 5. TPR profile (**a**) ZA3S4 and ZA3L1, (**b**) ZH3S3 and ZH3L1.

Table 3 shows the temperatures at which the maximum reduction peaks identified occurred for each catalyst. The moles of H$_2$ consumed per gram of catalyst are shown in Table 4, in which that corresponding to the catalyst ZA3S4 was the highest consumption of H$_2$ (6.403 mmol H$_2$/g). This is interpreted as the greater amount of copper present in this catalyst with respect to the others; it is observed that this result agrees with the elemental analysis results presented previously (% w Cu of 5.36%).

Table 3. Reduction temperatures of the Cu/zeolite ZSM-5 catalysts.

Peak No.	Reduction Temperatures (°C)			
	ZA3S4	**ZA3L1**	**ZH3S3**	**ZH3L1**
1	145.9	140.0	246.5	409.1
2	224.4	203.6	471.7	455.5
3	435.0	378.7	-	-

Table 4. H_2 consumed during TPR analysis on Cu/ZSM-5 catalysts.

Catalyst	mmol H_2	mmol H_2/g
ZA3S4	0.452	6.403
ZA3L1	0.217	3.098
ZH3S3	0.232	3.313
ZH3L1	0.014	0.206

The lower reduction temperatures of the catalysts obtained by LPIE with respect to the catalysts obtained by SSIE (Table 3) is attributed to a lower binding force of Cu^{2+} with the zeolite matrix; while, in the case of catalysts obtained by the SSIE method, the exchange is carried out mainly by gaseous diffusion of the metal through the pores, which allows the exchange of Cu within the less accessible sites and therefore requires higher temperatures for its reduction.

Regarding the copper species present, it is known that for low metal contents, the main species is Cu^{2+}, which can be reduced in two steps to Cu^0. The reduction of Cu^{2+} to Cu^+ occurs at low temperatures, while the reduction of Cu^+ to Cu^0 occurs at higher temperatures [27]. According to previous studies by Tounsi et al. and Delahay et al. [25,28], the reactions involved in the reduction process of copper-exchanged zeolites are the following:

$$CuO + H_2 \rightarrow Cu^0 + H_2 \tag{1}$$

$$Cu^{2+} + H_2 \rightarrow Cu^+ + 2H^+ \tag{2}$$

$$Cu^+ + H_2 \rightarrow Cu^0 + 2H^+ \tag{3}$$

Based on the above, in the case of the ZA3S4 and ZA3L1 catalysts, the Cu^{2+} species reduced to Cu^+ are associated with the first observed peak (reaction (2)), Cu^{2+} in CuO species reduced to Cu^0 with the second peak (reaction (1)) and species Cu^+ to Cu^0 withthe third peak (reaction (3)) [25].

On the other hand, for the ZH3S3 catalyst, the peak of 246.5 °C is associated with the reduction of Cu^{2+} ions to Cu^+ (reaction (2)) and the second peak at 471.7 °C corresponds to the reduction of Cu^+ to Cu^0 (reaction (3)). Finally, for the ZH3L1 catalyst, the peaks greater than 350 °C correspond to the reduction of Cu^+ to Cu^0 [21,29].

4. Conclusions

The results show that the synthesis method of the catalysts established a difference in the resulting physical-chemical properties of each one. The EDS analyses showed that the catalysts obtained by SSIE exhibited a higher copper load than those obtained by LPIE, which is attributed to the fact that SSIE facilitates the diffusion of the volatile copper metal complex through the interior pores of the zeolite. The highest copper content was reached in the ZA3S4 catalyst (5.36% by weight), which was obtained by SSIE with the zeolite in ammonia form.

On the other hand, the XRD results show no difference between the catalysts and their reference standard, except for the ZH3S3 catalyst in which the characteristic diffraction lines of metallic copper are observed.

In the case of the FTIR analysis, the characteristic absorption bands of the ZSM-5 zeolite were observed for all the catalysts; however, it is not possible to visualize other

absorption bands in the studied region that may be associated with the incorporation of the metal. Finally, by means of the TPR analysis, three peaks corresponding to the reduction of copper in the catalysts were obtained with ammonia zeolite, and two reduction peaks for the catalysts obtained with the zeolite in acid form were identified. The peaks correspond to the reduction of Cu^{2+} to Cu^+, CuO to Cu^0, and Cu^+ to Cu^0, in order of increasing temperature. The lower temperature reduction peaks were for the catalysts obtained by LPIE, rather than for those obtained by SSIE.

The results found suggest that the two ion exchange methods are suitable for incorporating Cu with a homogeneous distribution into the zeolite structure, with SSIE being the one that provides the highest exchange percentage. These catalysts can be used in the transformation of methane to methanol and the catalytic hydrogenation of CO_2 through a hybrid catalyst.

Author Contributions: D.S.C.-N. carried out the experimental work of synthesis of the Cu/ZSM-5 catalysts by two ion exchange methods, M.G.-A. tested and interpreted the SEM/EDS analysis of catalysts, V.M.-Á. conducted the discussion of results, M.T.-R. and S.B.P. participated in the direction and discussion of the results. All authors have read and agreed to the published version of the manuscript.

Institutional Review Board Statement: Not applicable.

Informed Consent Statement: Not applicable.

Data Availability Statement: Data are contained within the article.

Conflicts of Interest: The authors declare no conflict of interest.

References

1. Breck, D.W. *Zeolite Molecular Sieves: Structure, Chemistry and Use*; John Wiley & Sons: Hoboken, NJ, USA, 1974.
2. Yang, H.; Zhang, C.; Gao, P.; Wang, H.; Li, X.; Zhong, L.; Wei, W.; Sun, Y. A review of the catalytic hydrogenation of carbon dioxide into value-added hydrocarbons. *Catal. Sci. Technol.* **2017**, *7*, 4580–4598. [CrossRef]
3. Perego, C.; Carati, A. Zeolites and zeolite-like materials in industrial catalysis. In *Zeolites: From Model Materials to Industrial Catalysts*; Transworld Research Network: Kerala, India, 2008; pp. 357–389.
4. Liu, X.M.; Lu, G.; Yan, Z.F.; Beltramini, J. Recent Advances in Catalysts for Methanol Synthesis via ydrogenation of CO and CO_2. *Ind. Eng. Chem. Res.* **2003**, *42*, 6518–6530. [CrossRef]
5. Perego, C.; Pierluigi, V. Catalyst preparation methods. *Catal. Today* **1997**, *34*, 281–305. [CrossRef]
6. Pinna, F. Supported metal catalysts preparation. *Catal. Today* **1998**, *41*, 129–137. [CrossRef]
7. Tamas, I.; Ganea, R.; Pop, G. Catalysts and reaction conditions screening by microreactor devices for exhaust gas purification. In *Microreaction Technology*; Springer: Berlin/Heidelberg, Germany, 2001; pp. 464–469.
8. Campanati, M.; Fornasari, G.; Vaccari, A. Fundamentals in the preparation of heterogeneous catalysts. *Catal. Today* **2003**, *77*, 299–314. [CrossRef]
9. Shwan, S.; Skoglundh, M.; Lundegaard, L.; Tiruvalam, R.; Janssens, T.; Carlsson, A.; Vennestrøm, P. Solid-state ion-exchange of copper into zeolites facilitated by ammonia at low temperature. *ACS Catal.* **2015**, *5*, 16–19. [CrossRef]
10. Jouini, H.; Mejri, I.; Petitto, C.; Martínez, J.; Vidal, A.; Mhamdi, M.; Blasco, T.; Delahay, G. Characterization and NH_3-SCR reactivity of Cu-Fe-ZSM-5 catalysts prepared by solid state ion exchange: The metal exchange order effect. *Microporous Mesoporous Mater.* **2018**, *260*, 217–226. [CrossRef]
11. Abu, B.; Schwieger, W.; Unger, A. Nitrous oxide decomposition over transition metal exchanged ZSM-5 zeolites prepared by the solid-state ion exchange method. *Appl. Catal. B Environ.* **2008**, *84*, 277–288.
12. Gates, B.C.; Flytzani-Stephanopoulos, M.; Dixon, D.A.; Katz, A. Atomically dispersed supported metal catalysts: Perspectives and suggestions for future research. *Catal. Sci. Technol.* **2017**, *7*, 4259–4275. [CrossRef]
13. Gates, B.C. Atomically Dispersed Supported Metal Catalysts: Seeing Is Believing. *Trends Chem.* **2019**, *1*, 99–110. [CrossRef]
14. Chen, Y.; Li, H.; Zhao, W.; Zhang, W.; Li, J.; Li, W.; Zheng, X.; Yan, W.; Zhang, W.; Zhu, J.; et al. Optimizing reaction paths for methanol synthesis from CO_2 hydrogenation via metal-ligand cooperativity. *Nat. Commun.* **2019**, *10*, 1885. [CrossRef] [PubMed]

15. Chen, L.; Jansson, J.; Skoglundh, M.; Grönbeck, H. Mechanism for Solid-State Ion Exchange of Cu+ into Zeolites. *J. Phys. Chem. C* **2016**, *120*, 29182–29189. [CrossRef]

16. Zhang, Y.; Briggs, D.N.; de Smit, E.; Bell, A.T. Effects of zeolite structure and composition on the synthesis of dimethyl carbonate by oxidative carbonylation of methanol on Cu-exchanged Y, ZSM-5, and Mordenite. *J. Catal.* **2007**, *251*, 443–452. [CrossRef]

17. Anastas, P.; Kirchhoff, M.; Williamson, T. Catalysis as a foundational pillar of green chemistry. *Appl. Catal. A Gen.* **2001**, *221*, 3–13. [CrossRef]

18. International Zeolite Association. Database of Zeolite Structures. Structure Commission of the International Zeolite Association. 2017. Available online: http://america.iza-structure.org/IZA-SC/pow_pat.php?STC=MFI&ID=MFI_0 (accessed on 10 September 2021).

19. Natesakhawat, S.; Lekse, J.; Baltrus, J.; Ohodnicki, P.; Howard, B.; Deng, X.; Matranga, C. Active sites and structure−activity relationships of copper-based catalysts for carbon dioxide hydrogenation to methanol. *ACS Catal.* **2012**, *2*, 1667–1676. [CrossRef]

20. Li, S.; Guoa, L.; Ishiharab, T. Hydrogenation of CO_2 to methanol over Cu/AlCeO catalyst. *Catal. Today* **2020**, *339*, 352–361. [CrossRef]

21. Bulánek, R.; Wichterlová, B.; Sobalík, Z.; Tichý, J. Reducibility and oxidation activity of Cu ions in zeolites Effect of Cu ion coordination and zeolite framework composition. *Appl. Catal. B Environ.* **2001**, *31*, 13–25. [CrossRef]

22. Drake, I.J.; Zhang, Y.; Briggs, D.; Lim, B.; Chau, T.; Bell, A. The Local Environment of Cu^+ in Cu-Y Zeolite and Its Relationship to the Synthesis of Dimethyl Carbonate. *J. Phys. Chem. B* **2006**, *110*, 11654–11664. [CrossRef]

23. Li, C.; Wu, Z.; Auerbac, S.; Carrado, K.; Dutta, P. Microporous materials characterized by vibrational spectroscopies. In *Handbook of Zeolite Science and Technology*; CRC Press: Boca Raton, FL, USA, 2003; pp. 435–436.

24. Kulprathipanja, S. Zeolite Characterization. In *Zeolites in Industrial Separation and Catalysis*; John Wiley & Sons: Hoboken, NJ, USA, 2010; p. 114.

25. Tounsi, H.; Djemel, S.; Ghorbel, A.; Delahay, G. Characterization and performance of over-exchanged Cu-ZSM-5 catalysts prepared by solid-state ion exchange for the selective catalytic reduction of no by n-decane. *J. Société Chim. Tunis.* **2007**, *9*, 85–96.

26. Nanba, T.; Masukawa, S.; Ogata, A.; Uchisawa, J.; Obuchi, A. Active sites of Cu-ZSM-5 for the decomposition of acrylonitrile. *Appl. Catal. B Environ.* **2005**, *61*, 288–296. [CrossRef]

27. De Lucas, A.; Valverde, J.L.; Dorado, F.; Romero, A.; Asencio, I. Influence of the ion exchanged metal (Cu, Co, Ni and Mn) on the selective catalytic reduction of NOX over mordenite and ZSM-5. *J. Mol. Catal. A Chem.* **2004**, *225*, 47–58. [CrossRef]

28. Delahay, G.; Coq, B.; Broussous, L. Selective catalytic reduction of nitrogen monoxide by decane on copper-exchanged beta zeolites. *Appl. Catal. B Environ.* **1996**, *12*, 49–59. [CrossRef]

29. Urquieta González, E.; Martins, L.; Peguin, R.P.S.; Batista, M.S. Identification of Extra-Framework Species on Fe/ZSM-5 and Cu/ZSM-5 Catalysts Typical Microporous Molecular Sieves with Zeolitic Structure. *Mater. Res.* **2002**, *5*, 321–327. [CrossRef]